Acta Crystallographica Section F
Structural Biology and Crystallization Communications
ISSN 1744-3091

Structure of ribose 5-phosphate isomerase from *Plasmodium falciparum*

Margaret A. Holmes,[a,b] Frederick S. Buckner,[a,c] Wesley C. Van Voorhis,[a,c] Christophe L. M. J. Verlinde,[a,b] Christopher Mehlin,[a,b] Erica Boni,[a,b] George DeTitta,[a,d] Joseph Luft,[a,d] Angela Lauricella,[a,d] Lori Anderson,[a,b] Oleksandr Kalyuzhniy,[a,b] Frank Zucker,[a,b] Lori W. Schoenfeld,[a,b] Thomas N. Earnest,[a,e] Wim G. J. Hol[a,b,f] and Ethan A. Merritt[a,b]*

[a]Structural Genomics of Pathogenic Protozoa (SGPP) Consortium, USA, [b]Department of Biochemistry, University of Washington, Seattle, WA 98195-7742, USA, [c]Department of Medicine, University of Washington, Seattle, WA 98195, USA, [d]Hauptman–Woodward Institute, Buffalo, NY 14203, USA, [e]Lawrence Berkeley National Laboratory, Berkeley, CA 94720, USA, and [f]Howard Hughes Medical Institute, University of Washington, Seattle, WA 98195, USA

Correspondence e-mail: merritt@u.washington.edu

Received 18 February 2006
Accepted 24 March 2006

PDB Reference: ribose 5-phosphate isomerase, 2f8m, r2f8msf.

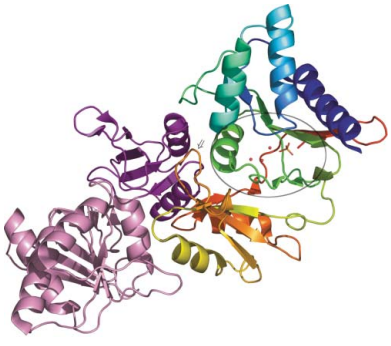

The structure of ribose 5-phosphate isomerase from *Plasmodium falciparum*, PFE0730c, has been determined by molecular replacement at 2.09 Å resolution. The enzyme, which catalyzes the isomerization reaction that interconverts ribose 5-phosphate and ribulose 5-phosphate, is a member of the pentose phosphate pathway. The *P. falciparum* enzyme belongs to the ribose 5-phosphate isomerase A family, Pfam family PF06562 (DUF1124), and is structurally similar to other members of the family.

1. Introduction

Ribose 5-phosphate isomerase (EC 5.3.1.6; Rpi) catalyzes the interconversion of the ketose ribose 5-phosphate and its isomer, the aldose ribulose 5-phosphate, in photosynthetic carbon fixation and in the pentose phosphate pathway, where it is used for purine- and pyrimidine-nucleoside synthesis and for histidine synthesis. The enzyme exists as two distinct proteins, RpiA and RpiB. Although RpiA and RpiB catalyze the same reaction, they show no sequence or overall structural homology. A number of RpiA and RpiB structures have been determined with and without ligands. RpiA is found in all three kingdoms of life and structures are available from *Escherichia coli*, *Haemophilus influenzae*, *Pyrococcus horikoshii*, *Saccharomyces cerevisiae* and *Thermus thermophilus*. RpiB is present in bacteria and also in the trypanosomatids (*Leishmania* spp., *Trypanosoma*) and related pathogenic eukaryotes (*Entamoeba histolytica*, *Giardia lamblia*). Structures of RpiB are only known from bacteria.

Searches against all *Plasmodium* spp. genomic sequences in the PlasmoDB sequence database (Bahl *et al.*, 2002) using the *TBLASTN* 2.1.2 protocol and the *E. coli*, *L. major* and *E. histolytica* RpiB gene sequences as probes found no plausible instances of a plasmodial RpiB gene. The only hit of marginal significance (E = 0.08) was against a *P. falciparum* chr 10 sequence annotated as 'rifin surface antigenic variant'. We therefore conclude that RpiA is the sole form of this enzyme present in plasmodia. The present structure determination of an RpiA from *P. falciparum* was undertaken as part of the SGPP (Structural Genomics of Pathogenic Protozoa Consortium; http://www.sgpp.org) effort targeting proteins from eukaryotic tropical pathogens.

2. Materials and methods

Ligase-independent cloning (Aslanidis & de Jong, 1990) was used to append a His tag to the N-terminus and a TAA stop codon to the C-terminus of the PFE0730c gene of *P. falciparum*, giving MAHHHHHH-orf-TAA (SGPP target identifier Pfal008434AAA). The vector has a T7 promoter for growth in *E. coli* with auto-induction media (without the use of IPTG). Selenomethionine protein was produced in *E. coli* strain BL21 DE3 Star according to the protocols of Studier (2005) and SGPP (Mehlin *et al.*, 2006).

Pfal008434AAA (8 mg ml^{-1}) was screened for crystallization conditions at the Hauptman–Woodward Institute high-throughput screening facility (Luft *et al.*, 2003). The protein was combined with 1536 different crystallization cocktail solutions in a single plate under mineral oil to prevent dehydration. Experiments were set up using

Table 1
Data-collection statistics.

Space group	$P2_12_12$
Unit-cell parameters (Å)	a = 93.7, b = 136.2, c = 45.0
Wavelength (Å)	1.03492
Resolution range (Å)	50–2.08 (2.14–2.08)
No. unique reflections	31605
Redundancy	5.9 (4.5)
Completeness (%)	92.7 (96.6)
R_{merge}	0.073 (0.368)
Mean $I/\sigma(I)$	26.5 (4.0)

Table 2
Refinement and model statistics.

Values in parentheses are for the highest resolution shell.

Resolution range (Å)	50–2.09 (2.14–2.09)
R_{work} (18076 reflections)	0.209 (0.280)
R_{free} (926 reflections)	0.272 (0.321)
R.m.s.d. bonds (Å) (*REFMAC* v.5.2.005)	0.017
R.m.s.d. angles (°)	1.625
Residues in most favored region of φ/ψ (*PROCHECK*)	400 [94.8%]
Residues in additional allowed region of φ/ψ	22 [5.2%]
Residues in generously allowed region of φ/ψ	0
Residues in disallowed region of φ/ψ	0
Mean B factor (Å^2), protein atoms (3555)	28.7
Mean B factor (Å^2), water molecules (226)	29.1
Mean B factor (Å^2), phosphate atoms (10)	41.6

standard commercially available liquid-handling systems. Plates were imaged over a four-week time course. Images were reviewed and crystallization conditions were forwarded to the crystal-growth laboratory in Seattle for optimization. There, crystallization conditions from the initial screen were optimized for pH, major precipitant and additive concentrations using a vapor-diffusion sitting-drop method. Crystallization conditions for the first crystal form were 100 m*M* NH_4SCN, 15% PEG 1000, 50 m*M* HEPES pH 8.2. The crystallization conditions for the crystal used for structure solution were 200 m*M* NaCl, 0.6 m*M* $KAu(CN)_2$, 20% PEG 3000, 100 m*M* HEPES pH 7.5 at 277 K. Both types of crystals were flash-frozen directly in liquid nitrogen prior to shipping for data collection.

The first crystal form grown of Pfal008434AAA was in space group *P*1, with 8–10 monomers predicted in the asymmetric unit based on V_M calculations (Matthews, 1968; later determined by searching with the refined structure to be eight monomers, giving a V_M of 2.8 Å^3 Da^{-1}). Molecular replacement using the program *EPMR* (Kissinger *et al.*, 1999) and monomer search models from PDB entries 1uj5 (*T. thermophilus*) and 1lk7 (*P. horikoshii*) did not succeed. Attempts to phase using SeMet MAD data from the same crystal form were also unsuccessful. In an effort to find a heavy-atom derivative, the protein was cocrystallized with $KAu(CN)_2$ and diffraction data were collected at the Au peak wavelength at the Advanced Light Source beamline 8.2.1. The data were integrated and scaled using *HKL*2000 (Otwinowski & Minor, 1997). There was no evident anomalous scattering signal that would indicate incorporation of Au, but the protein had crystallized in a different space group, $P2_12_12$, with two monomers in the asymmetric unit, giving a V_M of 2.6 Å^3 Da^{-1}. The structure was solved by molecular replacement, using the program *EPMR* and a monomer from 1uj5, *T. thermophilus* RpiA (Hamada *et al.*, 2003), as the search model. The asymmetric unit contains one dimer of RpiA. Alternating rounds of modelling using the program *XFIT* (McRee, 1999) and refinement using the program *REFMAC*5 (Murshudov *et al.*, 1997) *via* the *CCP4i* interface (Potterton *et al.*, 2004) were carried out. Non-crystallographic symmetry restraints were not used. Refinement was monitored using 5% of the data reserved for R_{free}. Final structure validation was performed with *PROCHECK* (Laskowski *et al.*, 1993), *MOLPROBITY* (Lovell *et al.*, 2003) and *COOT* (Emsley & Cowtan, 2004). The model of the *A* chain consists of the last four residues of the His tag and residues 1–233 of the 236-residue open reading frame. The model of the *B* chain consists of residues 1–235. No density corresponding to Au atoms was seen, but a phosphate ion was clearly visible in each of the two active sites.

3. Results and discussion

The structure of Pfal008434AAA has been solved to 2.09 Å. Data-collection statistics are shown in Table 1 and refinement statistics are shown in Table 2. The enzyme crystallizes with a dimer in the asymmetric unit; a ribbon drawing of the dimer is shown in Fig. 1. *P. falciparum* RpiA has 40% sequence identity over a 222-residue span with the search model from *T. thermophilus*; sequence identity with the other previously determined RpiA structures ranges from 31 to 36%. The human RpiA enzyme, the structure of which has not been determined, also falls in this range, with a sequence identity of 35%. As expected from the level of sequence identity with the other structures, Pfal008434AAA adopts the canonical RpiA fold. The RpiA monomer is a mixed $\alpha\beta$ protein which consists of two domains of unequal size. The larger domain is comprised of two stretches of chain, residues 1–129 and 210–236, and the smaller domain is comprised of the intervening stretch, residues 130–209. The active site

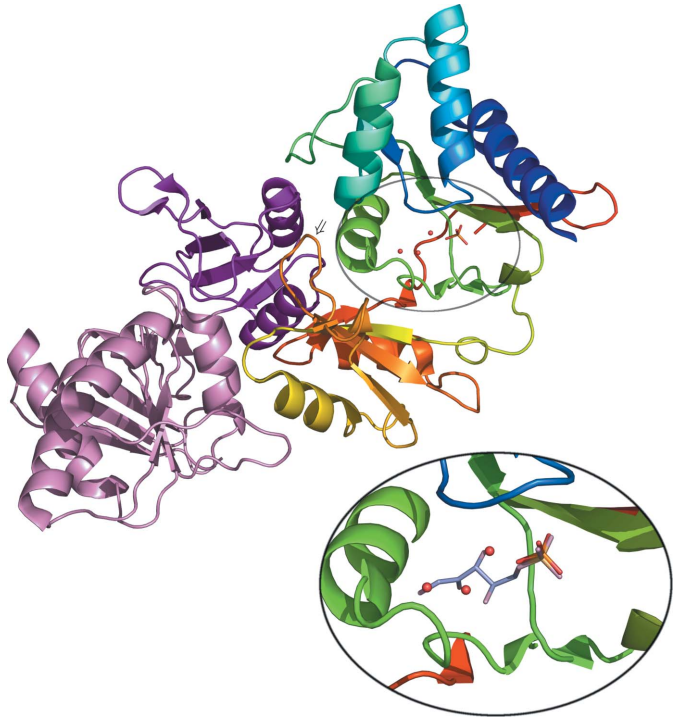

Figure 1
Main figure: ribbon representation of the Pfal008434AAA dimer. The *A* chain is colored smoothly from blue at the N-terminus to red at the C-terminus. The *B* chain is colored by domain, with the larger domain in pink and the smaller domain in purple. The tetramerization loop of chain *A* is indicated by an arrow. Inset: enlarged view of the active site of the Pfal008434AAA *A* chain. The bound phosphate ion is shown in stick form and the three water molecules mentioned in the text are indicated as spheres. The substrate ribose 5-phosphate (light blue) from the *T. thermophilus* structure 1uj5 is shown superposed onto the Pfal008434AAA active site based on superposition of 27 C^α atoms in two stretches of chain that contain ten of the 11 residues directly in contact with the ribose 5-phosphate. The figure was generated using *PyMOL* (DeLano, 2002).

is located in the larger domain and the 'tetramerization loop' (see below) is part of the smaller domain. The two monomers superimpose with an r.m.s. difference of 0.41 Å for 233 C^{α} atoms. The largest differences between the two chains, up to 2.8 Å, are in a loop in the large domain and are seen for residues 75–78, which are involved in crystal-packing interactions.

In the present structure, there is a phosphate ion bound in the active site of each monomer (Fig. 1, inset). Phosphate ion is a weak inhibitor (K_i = 7.9 m*M*) of spinach chloroplast RpiA (Jung *et al.*, 2000). Phosphate was not present in the protein buffer or crystallization solutions; presumably, it was acquired by the enzyme during protein expression. A phosphate ion was previously seen bound to the active site of RpiB from *Mycobacterium tuberculosis*, for which it is also a weak inhibitor (K_i = 130 m*M*; Roos *et al.*, 2004), but that protein was crystallized from sodium/potassium phosphate. Phosphate ions have not been seen in the active sites of previously determined RpiA structures. In our model, the phosphate ion is in the same location as the phosphate of ribose 5-phosphate in the *T. thermophilus* structure 1uj5 and participates in the same five direct phosphate–protein hydrogen bonds. In the 1uj5 structure, the phosphate O atoms also form hydrogen bonds to six water molecules; three of those water molecules are modelled in our structure and they interact similarly with the phosphate ion. The Pfal008434AAA active site also contains three additional water molecules. These are located at roughly the positions of the ribose hydroxyl O atoms O1, O2 and O3 and form the same hydrogen bonds to the protein as the ribose O atoms, although with slightly different geometry.

Members of the RpiA family exist in two oligomerization states, as observed in the structures determined thus far. The bacterial RpiAs (*E. coli*, *H. influenzae*, *T. thermophilus*) form dimers (Rangarajan *et al.*, 2002; Zhang *et al.*, 2003; Hamada *et al.*, 2003; K. Das, R. Xioa, T. Acton, G. Montelione & E. Arnold, PDB code 1m0s), while the archaeal (*Py. horikoshii*) and eukaryotic (*S. cerevisiae*) enzymes form tetramers (Ishikawa *et al.*, 2002; Graille *et al.*, 2005). However, the *P. falciparum* structure presented here is observed in the crystal as a dimer. Furthermore, in the size-exclusion chromatography step of protein purification, the protein ran as a dimer (98%) with a minor 74 kDa peak (1%) that may correspond to a tetramer. Only the major peak fraction was taken into crystallization trials. The RpiA oligomerization state has been postulated (Ishikawa *et al.*, 2002; Graille *et al.*, 2005) to be determined by the length of what could be called the 'tetramerization loop'. Yeast and other eukaryotes typically have 16–17 residues in this loop, as do the archaea. In previously observed structures containing this longer loop, it has a conformation which allows interaction with the same loop of a second dimer to form a tetramer. The equivalent loop is shorter in the dimeric bacterial structures. The *P. falciparum* loop is 14 residues long. Structure-based sequence alignment of the *P. falciparum* sequence with bacterial, archaeal and eukaryotic sequences shows that Pfal008434AAA has the shorter loop seen in bacterial forms of the enzyme, consistent with the dimer being the predominant form in solution (Fig. 2).

The extent and nature of the RpiA active site are known from previous paired apo and substrate-bound structures from *T. thermophilus*, *Py. horikoshii* and *E. coli*. It is noteworthy that there

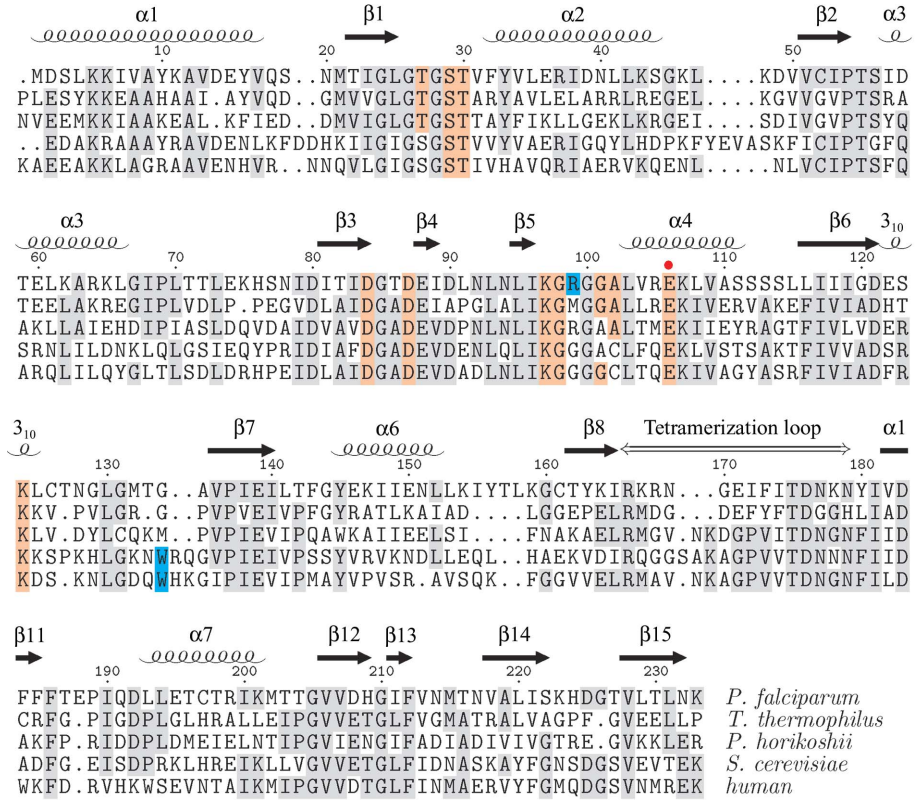

Figure 2
Structure-based sequence alignment of ribose 5-phosphate isomerase RpiA from *P. falciparum* (2f8m), *T. thermophilus* (1uj5), *Py. horikoshii* (1lk5) and *S. cerevisiae* (1xtz). Residue numbering and secondary-structure elements are those of the present structure. The alignment was produced by the CEMC server (Guda *et al.*, 2001, 2004). The human RpiA sequence, for which no structure has yet been reported, was added separately. Conserved residues that directly contact the ribose 5-phosphate in the 1uj5 structure are indicated by colored shading and the proposed general base/acid (Glu106 in *P. falciparum*) is indicated by a red dot (Ishikawa *et al.*, 2002; Zhang *et al.*, 2003; Hamada *et al.*, 2003). Residues contributing to a significantly different binding site surface in the *P. falciparum* and human enzymes are highlighted in cyan. The figure was generated using *T_EXshade* (Beitz, 2000).

are no significant conformational changes in active-site residue conformations between the apo (PDB code 1uj4) and substrate-bound (PDB code 1uj5) *T. thermophilus* structures (Hamada *et al.*, 2003). Conformational changes at the active site upon D-4-phosphoerithronic acid binding to the *Py. horikoshii* enzyme (Ishikawa *et al.*, 2002) and upon arabinose-5-phosphate binding to the *E. coli* enzyme are also observed to be minimal (Rangarajan *et al.*, 2002; Zhang *et al.*, 2003). The location of the phosphate moiety is consistent in all of these complexes and in the current structure.

A detailed comparison of the corresponding active-site residues in the *P. falciparum* and human RpiA protein sequences revealed an unexpected difference. Near the 4-hydroxyl of ribose-5-phosphate, the position of which is inferred from the structure of the *T. thermophilus* complex (PDB code 1uj5), the active site is lined by a loop between β5 and α4. This loop has sequence KGRGGA in the *Plasmodium* enzyme, while the sequence is KGGGGC in the human enzyme (Fig. 2). There is no crystal structure of the human enzyme, but the *S. cerevisiae* enzyme structure (PDB code 1xtz) is 45% identical in sequence and provides the basis for a homology model illuminating a potentially exploitable difference in binding-site features at this point. The human and yeast enzymes contain a short insertion relative to the *P. falciparum* sequence near residue 135 (Fig. 2). Surprisingly, the space occupied by Arg99 in the *Plasmodium* enzyme structure is instead occupied by a tryptophan side chain in the yeast structure, originating from a loop between β6 and β7 (Fig. 3). Although the homologous Arg residue in *P. horikoshii* is not required for enzyme activity (Ishikawa *et al.*, 2002), this Arg *versus* Trp difference may provide a basis for the design of selective inhibitors of the parasite enzyme. Chemical substituents that favor a polar interaction or hydrogen bond with the Arg99 side chain of the binding site of the *P. falciparum* enzyme will not be so favored by the purely hydrophobic face of Trp134 in the human enzyme's binding site.

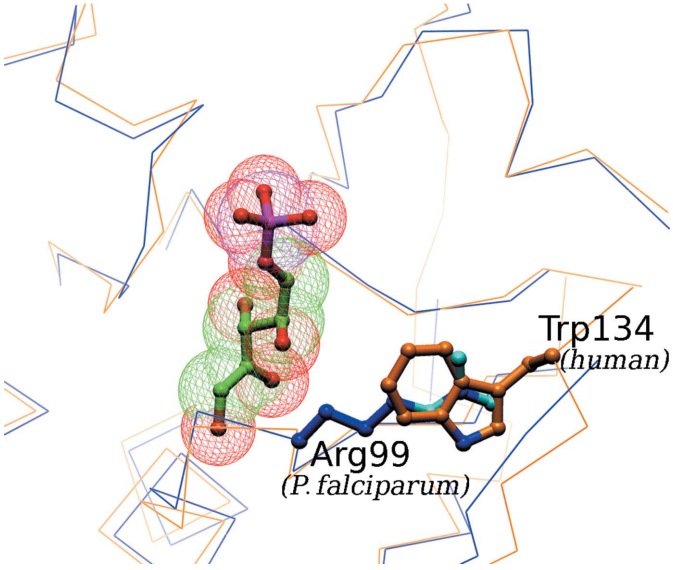

Figure 3
Potentially exploitable difference in the ribose-5-phosphate-binding site in the *P. falciparum* and human RpiA proteins. The blue backbone trace in the figure is that of the *P. falciparum* structure presented here; the gold trace is that of a homology model for the human RpiA based on the crystal structure (1xtz) of the yeast homolog. The ribose-5-phosphate substrate is positioned as seen in the *T. thermophilus* enzyme–substrate complex (1uj5). The very different binding-site environment to the right of the substrate, Arg99 in *P. falciparum* and Trp134 in humans (Trp157 in yeast), suggests that it would be possible to design inhibitors with very different affinities for the two homologous enzymes.

The structure presented here is the second structure determination of a eukaryotic ribose 5-phosphate isomerase. This enzyme is essential in the model eukaryote *S. cerevisiae* (Giaever, 2002). Its role in *Plasmodium* biology has not been evaluated using knockout technology, but owing to its central role in the pentose phosphate pathway, RpiA is likely to be essential in *P. falciparum*. The pentose phosphate pathway serves two critical cellular functions: it generates NADPH for reducing power and it produces ribose-5-phosphate, the sugar component of nucleic acids. *Plasmodium* cells have a critical need for an abundant supply of reducing power in order to sustain their rapid growth and to detoxify heme, the product of hemoglobin digestion (Becker *et al.*, 2003). *Plasmodium* also has an intense requirement for nucleic acid production to support its rapid proliferation. In fact, the ribose product of the pentose phosphate shunt (5-phospho-D-ribose 1-pyrophosphoric acid) that goes into nucleic acids is increased 56-fold in concentration in infected erythrocytes compared with uninfected erythrocytes (Roth *et al.*, 1986). It follows that ribose 5-phosphate isomerase is likely to be a good chemotherapeutic target for *Plasmodium*.

We are grateful for the contributions of other SGPP consortium members, including Peter Myler, Elizabeth Worthey, Helen Neeley, Tracy Arakaki, Jürgen Bosch, Jonathan Caruthers, Mark A. Robien, Larry de Soto and Martin Criminale. We also thank Michael H. Gelb. Portions of this work were carried out at the Advanced Light Source, which is supported by the Director, Office of Science, Office of Basic Energy Sciences of the US Department of Energy under Contract No. DE-AC02-05CH11231. This work was supported by NIH awards GM64655 and GM62617.

References

Aslanidis, C. & de Jong, P. J. (1990). *Nucleic Acids Res.* **18**, 6069–6074.
Bahl, A., Brunk, B., Coppel, R. L., Crabtree, J., Diskin, S. J., Fraunholz, M. J., Grant, G. R., Gupta, D., Huestis, R. L., Kissinger, J. C., Labo, P., Li, L., McWeeney, S. K., Milgram, A. J., Roos, D. S., Schug, J. & Stoeckert, C. J. Jr (2002). *Nucleic Acids Res.* **30**, 87–90.
Becker, K., Rahlfs, S., Nickel, C. & Schirmer, R. H. (2003). *Biol. Chem.* **384**, 551–566.
Beitz, E. (2000). *Bioinformatics*, **16**, 135–139.
DeLano, W. (2002). *The PyMOL Molecular Graphics System.* http://www.pymol.org.
Emsley, P. & Cowtan, K. (2004). *Acta Cryst.* D**60**, 2126–2132.
Giaever, G. *et al.* (2002). *Nature (London)*, **418**, 387–391.
Graille, M., Meyer, P., Leulliot, N., Sorel, I., Janin, J., Tilbeurgh, H. V. & Quevillon-Cheruel, S. (2005). *Biochimie*, **87**, 763–769.
Guda, C., Lu, S., Scheeff, E. D., Bourne, P. E. & Shindyalov, I. N. (2004). *Nucleic Acids Res.* **32**, W100–W103.
Guda, C., Scheeff, E. D., Bourne, P. E. & Shindyalov, I. N. (2001). *Pac. Symp. Biocomput.* **6**, 275–286.
Hamada, K., Ago, H., Sugahara, M., Nodake, Y., Kuramitsu, S. & Miyano, M. (2003). *J. Biol. Chem.* **278**, 49183–49190.
Ishikawa, K., Matsui, I., Payan, F., Cambillau, C., Ishida, H., Kawarabayasi, Y., Kikuchi, H. & Roussel, A. (2002). *Structure*, **10**, 877–886.
Jung, C. H., Hartman, F. C., Lu, T. Y. & Larimer, F. W. (2000). *Arch. Biochem. Biophys.* **373**, 409–417.
Kissinger, C. R., Gehlhaar, D. K. & Fogel, D. B. (1999). *Acta Cryst.* D**55**, 484–491.
Laskowski, R., MacArthur, M., Moss, D. & Thornton, J. (1993). *J. Appl. Cryst.* **26**, 283–291.
Lovell, S., Davis, I., Arendall, W. B. III, de Bakker, P., Word, J., Prisant, M., Richardson, J. & Richardson, D. (2003). *Proteins*, **50**, 437–450.
Luft, J. R., Collins, R. J., Fehrman, N. A., Lauricella, A. M., Veatch, C. K. & DeTitta, G. T. (2003). *J. Struct. Biol.* **142**, 170–179.
McRee, D. E. (1999). *J. Struct. Biol.* **125**, 156–165.
Matthews, B. W. (1968). *J. Mol. Biol.* **33**, 491–497.

Mehlin, C., Boni, E., Buckner, F. S., Engel, L., Feist, T., Gelb, M., Haji, L., Kim, D., Liu, C., Mueller, N., Myler, P. J., Reddy, J. T., Sampson, J. N., Subramanian, E., Van Voorhis, W. C., Worthey, E., Zucker, F. & Hol, W. G. J. (2006). In the press.
Murshudov, G. N., Vagin, A. A. & Dodson, E. J. (1997). *Acta Cryst.* D**53**, 240–255.
Otwinowski, Z. & Minor, W. (1997). *Methods Enzymol.* **276**, 307–326.
Potterton, L., McNicholas, S., Krissinel, E., Gruber, J., Cowtan, K., Emsley, P., Murshudov, G. N., Cohen, S., Perrakis, A. & Noble, M. (2004). *Acta Cryst.* D**60**, 2288–2294.
Rangarajan, E. S., Sivaraman, J., Matte, A. & Cygler, M. (2002). *Proteins*, **48**, 737–740.
Roos, A. K., Andersson, C. E., Bergfors, T., Jacobsson, M., Karlen, A., Unge, T., Jones, T. A. & Mowbray, S. L. (2004). *J. Mol. Biol.* **335**, 799–809.
Roth, E. F. Jr, Ruprecht, R. M., Schulman, S., Vanderberg, J. & Olson, J. A. (1986). *J. Clin. Invest.* **77**, 1129–1135.
Studier, F. W. (2005). *Protein Expr. Purif.* **41**, 207–234.
Zhang, R., Andersson, C. E., Savchenko, A., Skarina, T., Evdokimova, E., Beasley, S., Arrowsmith, C. H., Edwards, A. M., Joachimiak, A. & Mowbray, S. L. (2003). *Structure*, **11**, 31–42.